The tyrosine phosphatase DEP-1 induces cytoskeletal rearrangements, aberrant cell-substratum interactions and a reduction in cell proliferation

Stuart Kellie[1,2,*], Graham Craggs[2,4], Ian N. Bird[2,5] and Gareth E. Jones[3]

[1]School of Molecular and Microbial Sciences, Institute for Molecular Bioscience and CRC for Chronic Inflammatory Diseases, University of Queensland, Brisbane, QLD 4072, Australia
[2]Yamanouchi Research Institute, Littlemore Park, Armstrong Road, Oxford OX4 4XS, UK
[3]Randall Centre, King's College London, New Hunt's House, Guy's Campus, London SE1 1UL, UK
[4]OSI Pharmaceuticals, Watlington Road, Oxford, OX4 6LT, UK
[5]Oxford Glycosciences plc, The Forum, 86 Milton Park, Abingdon, Oxon OX14, UK
*Author for correspondence (e-mail: s.kellie@mailbox.uq.edu.au)

Accepted 12 September 2003
Journal of Cell Science 117, 609-618 Published by The Company of Biologists 2004
doi:10.1242/jcs.00879

Summary

The receptor protein tyrosine phosphatase density-enhanced phosphatase-1 (DEP-1) has been implicated in aberrant cancer cell growth and immune cell function, however, its function within cells has yet to be properly elucidated. To investigate the cellular function of DEP-1, stable cell lines inducibly expressing DEP-1 were generated. Induction of DEP-1 expression was found to decrease PDGF-stimulated tyrosine phosphorylation of a number of cellular proteins including the PDGF receptor, and to inhibit growth factor-stimulated phosphorylation of components of the MAPK pathway, indicating that DEP-1 antagonised PDGF receptor signalling. This was supported by data showing that DEP-1 expression resulted in a reduction in cell proliferation. DEP-1-expressing cells had fewer actin-containing microfilament bundles, reduced vinculin and paxillin-containing adhesion plaques, and were defective in interactions with fibronectin. Defective cell-substratum adhesion correlated with lack of activation of FAK in DEP-1-expressing cells. Time-lapse interference reflection microscopy of live cells revealed that although small focal contacts at the leading edge were generated in DEP-1-expressing cells, they failed to mature into stable focal adhesions, as found in control cells. Further motility analysis revealed that DEP-1-expressing cells retained limited random motility, but showed no chemotaxis towards a gradient of PDGF. In addition, cell-cell contacts were disrupted, with a change in the localisation of cadherin from discrete areas of cell-cell contact to large areas of membrane interaction, and there was a parallel redistribution of β-catenin. These results demonstrate that DEP-1 is a negative regulator of cell proliferation, cell-substratum contacts, motility and chemotaxis in fibroblasts.

Movies available on-line

Key words: Tyrosine phosphatase, Cytoskeleton, Motility.

Introduction

Tyrosine phosphorylation is central to many aspects of cellular responses to extracellular stimuli, including the transduction of signals from the cell surface to the nucleus, new gene expression, proliferation and cytoskeletal changes (Schlessinger, 2000; Hubbard and Till, 2000). Protein-tyrosine phosphatases (PTPs) act both as positive and negative regulators of signal transduction and members of the PTP family have essential functions in growth, differentiation and related responses in different cell types (Östman and Böhmer, 2001; Andersen et al., 2001). For example, CD45 is essential for the activation of the tyrosine kinase lck and downstream signalling of the T cell receptor (Chen et al., 1996); the intracellular PTP SHP-1 is a negative regulator of NK cell signalling (Binstadt et al., 1996), and PTP1B has been identified as a negative regulator of insulin signalling (Elchebly et al., 1999). DEP-1 (also known as CD148, HPTPh, Byp and rDEP-1) is a Class III receptor-like protein tyrosine phosphatase (R-PTP), which contains a single intracellular catalytic domain and a number of FNIII repeats in its extracellular domain.

Its molecular mass varies (180-250 kDa) because of variable glycosylation and it has been proposed to be a chondroitin sulphate proteoglycan. DEP-1 is expressed throughout the haematopoietic system and in a wide variety of tissues including pancreas, thyroid, kidney, mammary gland and nervous system (Autschbach et al., 1999; de la Fuente-Garcia, 1998). DEP-1 is expressed at low levels in resting T cells, but is upregulated in activated T cells, and ligation with anti-DEP-1 antibodies induces proliferation of anti-CD3 activated T cells (Tangye et al., 1998a). Interestingly, transient transfection of DEP-1 has been reported to be a negative regulator of T cell activation, and also results in a reduction of TCR-mediated ERK-1 and ERK-2 activation, and reduced tyrosine phosphorylation (Palou et al., 1997; Hundt et al., 1997; Tangye et al., 1998a; Tangye et al., 1998b; Billard et al., 2000; del Pozo et al., 2000). DEP-1

expression also inhibits TCR-mediated activation of ras and calcium, and it has been reported that PLCγ and LAT are potential downstream targets for activated DEP-1 (Baker et al., 2001). In the mouse, DEP-1 is expressed at highest levels in macrophages; it is downregulated by CSF-1 and upregulated by lipopolysaccharide (Osborne et al., 1998). Hence, DEP-1 may be a regulator of macrophage growth and/or activation.

In 3T3 fibroblasts, R-PTPase activity increases eightfold in dense cultures compared with sparse cultures. The finding that there is no change in PTPase activity in serum-starved cells and that the increase in R-PTP activity can be demonstrated only in contact inhibited cells grown to high density (Keane et al., 1996) has led to the suggestion that R-PTPases may play a role in contact inhibition of cell growth. DEP-1 expression has been observed to increase dramatically in epithelial cells as they become confluent and so it may represent a candidate molecule for negative regulation of cell proliferation (Ostman et al., 1994; Keane et al., 1996; Sorby et al., 1996). DEP-1 has recently been shown to dephosphorylate the PDGF receptor, and thus is a putative negative regulator of PDGF signaling (Kovalenko et al., 2000; Persson et al., 2002). Holsinger et al. (Holsinger et al., 2002) have shown an interaction between DEP-1 and $p120^{ctn}$. Recently DEP-1 has been mapped to colorectal tumour susceptibility loci in mice and humans (Rivenkamp et al., 2002). Despite these reports, there is still little data on the function of DEP-1 in cells, and its natural ligand is unknown. Since previous attempts to generate stable DEP-1-overexpressing cell lines have been unsuccessful, we have chosen to investigate the functional consequences of DEP-1 overexpression using inducible cell lines. In this paper we describe DEP-1-mediated changes in cell proliferation, adhesion, motility and cytoskeletal reorganization in NIH 3T3 cells.

Materials and Methods

Cell culture

Unless otherwise stated, all cell lines were obtained from the American Type Culture Collection and maintained at 37°C in a humidified 5% CO2 incubator. NIH3T3 cells were grown in Dulbecco's modified Eagle's medium supplemented with 10% fetal bovine serum, 2 mM L glutamine, 100 units/ml penicillin, and 100 mg of streptomycin (Life Technologies, Inc.).

Cloning of DEP-1 and generation of inducible cell lines

Full-length human DEP-1 gene was cloned by PCR from MCF7 cells and ligated into pGeneV5/His inducible expression vector (Invitrogen) as described by the manufacturer. This was then transfected into pSwitch-containing stable NIH3T3 cells (Invitrogen) using Lipofectamin 2000 (Invitrogen) and further stable cell lines were isolated by selection in 400 μg/ml zeocin as described by the manufacturer. Three clones are described in this report: 1A2, a control clone that contains an empty pGene vector, and clones 2C2 and 2D3 that express full-length DEP-1 when treated with mifepristone**.** Preliminary dose response and time course experiments indicated that treatment with 1 nM mifepristone for 3 hours then washing out gave optimal DEP-1 expression with no apparent nonspecific effects on cells. Protein expression was assessed by immunofluorescence or western blotting 24-48 hours after induction.

Western blotting and immunoprecipitation

Uninduced cells or cells induced for 24 hours were quiesced for 4 hours in serum-free medium, then stimulated with 50 ng/ml PDGF for 10 minutes. In some cases 1 μM LY294002 was added as a PI 3-kinase inhibitor. Cells were washed three times in ice-cold Tris-buffered saline and solubilised in Laemmli sample buffer. 10% denaturing SDS-PAGE-separated proteins from 10^5 cells were transferred to nitrocellulose filters (Schleicher and Schuell, Dassell, Germany) and, after blocking with 5% non-fat dried milk for 1 hour, the filters were overlaid with a 1:1000 dilution of anti-V5 (Sigma) containing 0.05% Tween 20 for 1 hour. The filters were washed three times in PBS/Tween 20 and overlaid with a peroxidase-conjugated goat anti-mouse Ig (Bio-Rad). The bands were detected using the ECL system (Amersham Pharmacia Biotech). Other primary antibodies used were anti-PDGF receptor (Upstate Biotechnology, Lake Placid, NY), anti-cadherin (Sigma), anti-phosphotyrosine 4G10 (Upstate Biotechnology, Lake Placid, NY), anti-phospho-ERK and anti-phosphoAkt (New England Biolabs, Hitchin UK) and anti-FAK (Sigma). Immune precipitation was performed as previously described (Wilson et al., 1995). Briefly, 10^7 cells were resuspended in 1 ml RIPA buffer (Tris-buffered saline pH 7.2, 1% Nonidet P40, 1% sodium deoxycholate, 1 mM EDTA, 100 mM sodium orthovanadate) and protease inhibitor cocktail at 100 μl per 10^7 cells) and gently mixed on a rotator at 4°C for 20 minutes. The lysate was precleared with 50 ml of a 50% slurry of agarose-conjugated protein-A/G and incubated on a rotator at 4°C for 45 minutes. Anti-PDGF receptor (5 μl/ml; Upstate Biotechnology) was added to the precleared cell lysate and incubated on a rotator at 4°C for 2 hours. 40 μl of a 50% slurry of protein-A agarose was added and incubated for 1 hour at 4°C on a rotator. Immunocomplex bound to protein-A/G agarose was then collected by pulse centrifugation for 5 seconds at 11,000 ***g*** and washed three times with ice-cold RIPA buffer, followed by resuspension in 60 μl of 2× SDS sample buffer and heating to 100°C for 5 minutes. Samples were centrifuged at 11,000 ***g*** to remove the beads, and supernatants were separated by SDS-PAGE. FAK immune precipitation and western blotting was performed as previously described (Wilson et al., 1995).

Immunocytochemistry and fluorescence microscopy

BrdU incorporation was measured essentially as previously described (Murray et al., 2000) with the following modifications. 2×10^4 cells were plated on to coverslips in the bottom of 24-well plates in the presence or absence of 1 nM mifepristine. 16 hours later the cells were quiesced for 4 hours in serum-free medium. Cells were then stimulated by the addition of 50 ng/ml PDGF in 0.1% FCS for 18 hours, with 10 μM BrdU labelling reagent (Roche BrdU detection kit 1) being added for the final hour. Staining for BrdU was performed as described by the manufacturer. NIH3T3 cells were plated onto acid-washed glass coverslips at 50% confluence and incubated overnight. Cells were washed for 5 minutes in phosphate-buffered saline; PBS) and then fixed in 4% paraformaldehyde in PBS for 20 minutes. After a further 5-minute wash in PBS, cells were incubated in PBS, 10% normal goat serum (NGS) and 0.2% Triton X-100 for 30 minutes. The cells were then incubated overnight at 4°C with murine monoclonal antibodies against V5, paxillin, vinculin, tubulin, cadherin or catenin (Sigma), each diluted 1: 500 in PBS and 1% NGS. Cells were washed four times for 5 minutes in PBS, 10% NGS and 0.2% Triton X-100 before Alexa 488-conjugated goat anti-mouse antibody (Molecular Probes) was applied at 1:200 dilution in PBS and 1% NGS for 1 hour. After four additional 5-minute washes in PBS, 10% NGS and 0.2% Triton X-100, the cells were immersed briefly in distilled water and mounted in S3023 fluorescent mounting medium (Dako). In some cases, F-actin was localised by treating the cells with a 1:500 dilution of Rhodamine phalloidin (Sigma). Cells were viewed using an Axiovert 135 microscope (Zeiss) coupled to a monochrome light source (Photonics Polychrome II). A series of optical scans through the *z* axis of the cells were captured using a Hamamatsu digital camera, and image deconvolution was performed with Openlab software (Improvision).

Cell attachment and spreading on fibronectin

Acid-treated coverslips were treated with 0.05 mg/ml bovine plasma fibronectin (Sigma) overnight at 4°C, washed twice in PBS and placed in 24-multiwell dishes. 5×10^4 cells were plated in serum-free DMEM and incubated at 37°C for 1 hour or 3 hours as indicated (Wilson et al., 1995). Living cells were photographed and the number of attached or spread cells per field of view under ×20 objective lens magnification were counted. Spread cells were defined as those cells that had lost their phase bright appearance and had readily distinguishable nucleus and cytoplasm.

Interference reflection microscopy

Interference reflection images were collected using a Zeiss Standard 18 microscope with an incident light fluorescence attachment housed in a constant temperature room set at 37°C. Exciter and barrier filters were removed from the LP420 reflector and replaced with a narrow band pass filter to isolate the 546 nm line of the mercury arc source. Coverslips with attached cells were placed onto glass chambers, sealed with wax and observed using a Zeiss 63× Neofluar Antiflex oil immersion objective, NA 1.25. In some experiments, images were collected every second for a period of 10 minutes. For long-term studies, images were collected at 60-second intervals for up to 1 hour. Time-lapse images were collected digitally using in-house software. Single frame TIFF images were extracted from TIFF stacks using a routine written in Mathematica 4.2. Images were processed. Briefly, overlay methods were used to summate the intensities of the black zones (focal adhesions) at the leading edges of selected fibroblasts as measured in pixels. To counteract the effects of cell migration, quantification of the lifetime of individual pixels was performed on four images collected at 10-minute intervals. By appropriate manipulation of grey levels (0, black; 63, dark grey; 127, medium grey, and 191, light grey), a composite image can be generated that spans the four binned images. Black pixels represent pixels which were occupied in all four images, dark grey pixels were present in three out of four frames, medium grey two out of four frames, and light grey pixels were only present in one frame. Black pixels therefore reflect regions of low adhesion turnover, whereas light grey pixels represent regions of high adhesion turnover. We have defined a persistence index, where the percentage of pixels present in just one or two of the four images are divided by the percentage present in three or four images. Such procedures can be shown graphically (Fig. 7B) to demonstrate the effective turnover rate of cell-matrix adhesions; the lower the value of the persistence index, the less stable the adhesions (M. Holt, University College London, UK and G. E. Jones, unpublished).

Chemotaxis assays

Chemotaxis was assessed by direct observation and recording of cell behaviour in stable concentration gradients of PDGF using the Dunn chamber chemotaxis chamber (Weber Scientific International; Division of Hawksley Technology; www.hawksley.co.uk). This apparatus permits speed, direction of migration and displacement of individual cells to be measured in relation to the direction of a diffusible gradient (Zicha et al., 1991). Details of the construction and calibration of Dunn chambers can be found elsewhere (Allen et al., 1998; Jones et al., 2000). The chamber was filled with medium and a coverslip (previously seeded with cells and subject to appropriate experimental manipulation to induce DEP-1 expression where required) was inverted and sealed onto the chamber. Medium containing PDGF at a concentration of 60 ng/ml was placed into the outer well of the chamber. Chambers were maintained at 37°C and frame grabbing time-lapse recording of cells located on the bridge of the Dunn chamber was started within 30 minutes of assembly. Images of cells were digitally recorded at a time-lapse interval of 10 minutes for 6 hours using Kinetic Imaging AQM System (Kinetic Imaging plc, Bromborough UK, www.kineticimaging.com). Cells were tracked and analysed as described previously (Allen et al., 1998; Sturge et al., 2002). Briefly, cell tracks were generated from the time-lapse images using the image-processing program Lucida (also from Kinetic Imaging), and the resulting tracks were tested for directional bias using the Rayleigh test for unimodal clustering of directions (Jones et al., 2000; Mardia, 1972) using customised notebooks written in Mathematica™ for Windows (Wolfram Research Inc., Champaign, IL, USA). Horizon plots generated by the Mathematic notebook are displayed as circular histograms, such that if statistically significant unimodal clustering of cell trajectories is found, a mean direction (arrow) and the 95% confidence interval for the data set (grey segment) are automatically generated and displayed. Cells that translocated less than 20 μm from their point of origin (the horizon boundary) were excluded from this analysis.

Results

Inducible expression of DEP-1 in 3T3 cells

Repeated attempts to generate stable transfectants of DEP-1 failed because of a lack of long term growth in selection medium. As an alternative strategy, DEP-1 was cloned into pGene vector and this construct was transfected into NIH3T3 cells expressing the pSwitch vector. Clones were then selected and screened for the expression of DEP-1 induced by mifepristone. Fig. 1 shows examples of these clones. 1A2 is a clone of pSwitch 3T3 control cells transfected with empty pGene vector. This clone showed no expression of DEP-1 in the presence or absence of mifepristone. In contrast, clones 2C2 and 2D3 showed inducible expression of DEP-1 after mifepristone treatment. The induced DEP-1 was localized mainly to the plasma membrane with some endoplasmic reticulum staining, as expected for a transmembrane polypeptide (Fig. 1, upper panels). Western blotting confirmed that the mifepristone-induced DEP-1 was expressed at the expected size for the full-length protein (Fig. 1 lower panel). Mifepristone had no effect on levels of endogenous DEP-1 in NIH3T3 cells as assessed by real time PCR (data not shown).

DEP-1 effects on cell proliferation

Cultures of DEP-1-expressing cells appeared to grow to lower densities than control cells (data not shown). To investigate this in more detail the effect of DEP-1 on cell proliferation was assayed using BrdU uptake. Control 1A2 cells showed the same level of BrdU uptake in the presence or absence of mifepristone (Fig. 2), with 33% of the cells showing nuclear BrdU under normal culture conditions. However, whilst 2D3 cells in the absence of mifepristone displayed a similar level of BrdU incorporation, induction of DEP-1 with mifespristone significantly reduced the number of cells incorporating BrdU, from 32% to 8% of the population (Fig. 2). Thus DEP-1-expression significantly reduced the number of cells entering S phase.

Growth factor signalling

To examine in more detail the role of DEP-1 in growth inhibition, the effects of DEP-1 expression on the PDGF-dependent signalling events were examined. Initial experiments were performed to confirm the activity of expressed DEP-1 in NIH 3T3 cells. Cells were quiesced and

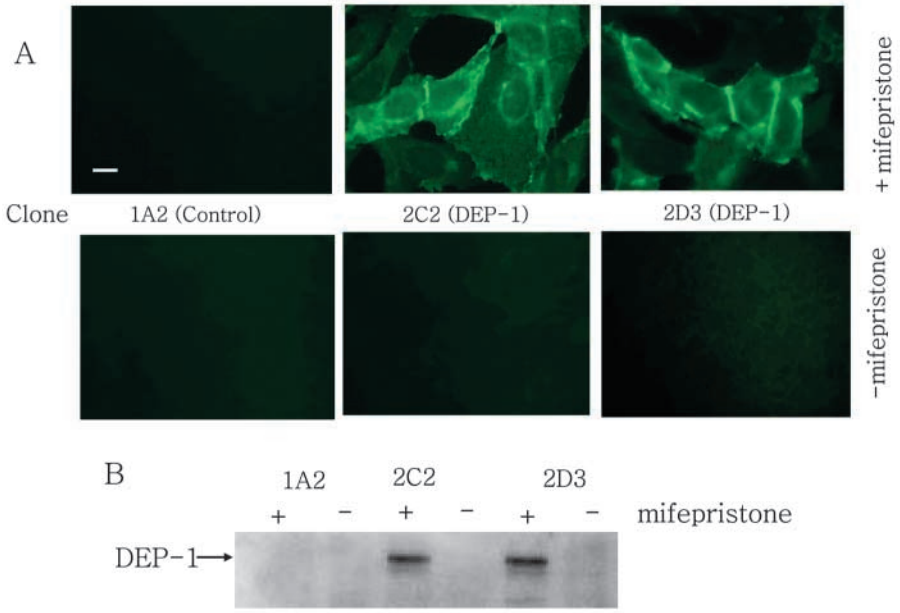

Fig. 1. Inducible expression of DEP-1 protein in NIH3T3 cells. (A) Immunofluorescent staining for DEP-1 in untreated or mifepristone-treated cells showing prominent plasma membrane and some ER localization. (B) Western blotting of DEP-1 in NIH3T3 cells showing full-length protein production. Scale bar: 10 μm.

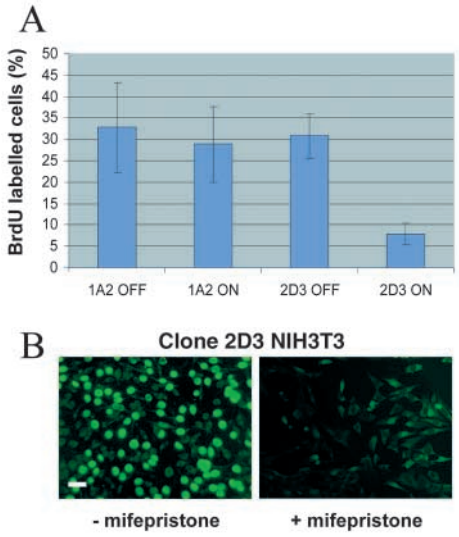

Fig. 2. DEP-1 expression causes cell cycle arrest. (A) Quantification of BrdU uptake in NIH3T3 cells. (B) Immunofluorescent staining for BrdU in 2D3 NIH3T3 cells (left) or 2D3 cells induced to express DEP-1 (right). Scale bar: 10 μm.

then stimulated with PDGF for 10 minutes. Phosphotyrosine blotting of whole cell lysates from quiesced or PDGF-stimulated cells demonstrated that the PDGF-stimulated increases in tyrosine phosphorylated polypeptides was suppressed in DEP-1-expressing cells (Fig. 3A). Immunoprecipitation confirmed the lack of ligand-induced tyrosine phosphorylation of the PDGF receptor in DEP-1-expressing cells (Fig. 3B). The role of DEP-1 in receptor signalling was further examined by investigating the association of c-*src* with the activated PDGF receptor. In unstimulated 1A2 control cells there was minimal association of c-*src* with PDGF receptor, however, after PDGF ligation c-*src* co-immunoprecipitated with the PDGF receptor (Fig. 3C). Mifepristone treatment had no effect on this response. Uninduced 2D3 cells displayed similar c-*src* association with activated PDGF receptor, but when DEP-1 was induced the association of c-*src* with activated PDGF receptor was ablated (Fig. 3C).

Quiescent 1A2 control cells showed the expected appearance of phosphorylated p42/p44 MAPK when stimulated with 50 ng/ml PDGF, and mifepristone had no effect on this, although it was inhibited as expected by the PI 3-kinase inhibitor LY294002 (Fig. 4A). In the absence of mifepristone, 2C2 and 2D3 cells also showed PDGF-dependent phosphorylation of p42/p44 MAPK. However, when these cells were induced to express DEP-1 the PDGF-dependent phosphorylation of p42/p44 MAPK was markedly reduced (Fig. 4A). Similarly, the appearance of phospho-Akt after PDGF simulation was not affected by mifepristone in 1A2 cells, but phospho-Akt generation was abolished by DEP-1 induction in 2D3 cells (Fig. 4B). These data suggest that DEP-1 inhibits cell growth by interfering with the ras-MAPK pathway and also the PI3-kinase-Akt pathway, leading to a reduction in proliferation and perhaps also cell survival. 2c2 cells showed similar responses to 2D3 cells.

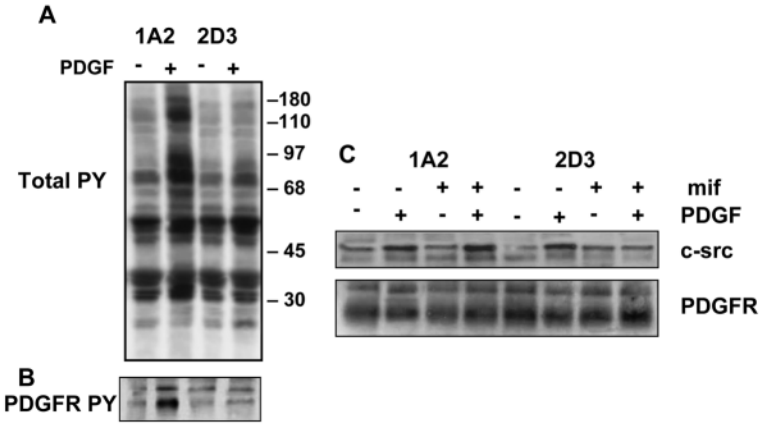

Fig. 3. DEP-1 expression reduces PDGF-induced tyrosine phosphorylation. Cells were quiesced for 4 hours then stimulated with 50 ng/ml PDGF. (A) Western blotting of whole cell lysates from PDGF-stimulated control 1A2 cells or DEP-1-expressing 2D3 cells with antiphosphotyrosine. (B) Western blotting of PDGF receptor immune precipitates with antiphosphotyrosine. (C) Association of c-*src* with PDGFR in DEP-1-expressing cells. DEP-1 expression reduces c-*src* association with PDGFR. Uninduced and induced NIH3T3 cells were stimulated with PDGF as described in Materials and Methods. PDGF receptor was immune precipitated and immunoblotted for c-*src* (upper panel) or PDGF (lower panel).

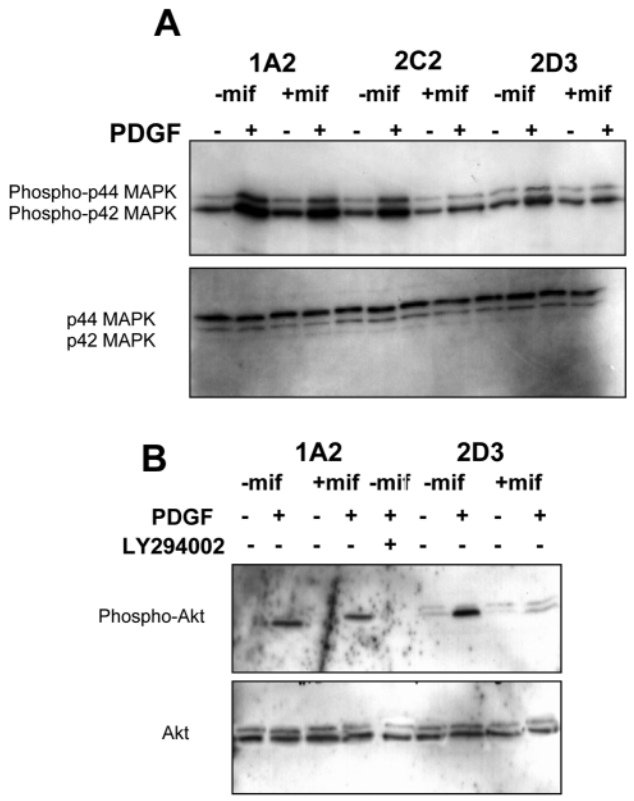

Fig. 4. DEP-1 expression reduces PDGF-induced MAP kinase and Akt phosphorylation. (A) Western blotting of NIH3T3-DEP-1 cells for phospho p42/p44 MAPK after quiescence and stimulation with PDGF. (B) Western blotting of NIH3T3-DEP-1 cells for phospho-akt after quiescence and stimulation with PDGF.

Cell-substratum interactions in DEP-1-expressing cells

The effects of DEP-1 expression on cell motility were examined by digital time-lapse photomicrography. Control 1A2 cells, in the presence of mifepristone, spread and polarised normally on tissue culture plastic. These cells showed the expected features of fibroblast motility including normal lamellipodia formation during polarised cell spreading (Fig. 5A). In contrast, mifepristone-treated 2C2 cells were much more rounded and showed a more random complex phenotype. The cells appeared to be tethered at one edge, which would periodically be released, resulting in intervals of relatively little vectoral movement followed by a sudden large jump of several microns (Fig. 5A; this is best seen in the accompanying movie, Movie 1, http://jcs.biologists.org.supplemental). The interactions of cells with a defined substratum was studied by quantifying the extent of cell spreading on fibronectin. Control 1A2 cells in the presence of mifepristone showed normal adhesion and spreading (defined by the lack of phase-bright cells as described in Materials and Methods), with progressively more cells adhering and spreading after 1 hour and 3 hours respectively. 2D3 cells expressing DEP-1 showed a lower number adherent cells and spread cells, only 50-60% that of control cells at both 1 hour and 3 hours (Fig. 5B). Unless otherwise stated, in all experiments uninduced 2D3 and 2C2 cells showed identical responses to uninduced 1A2 cells. FAK activation is a major downstream response to fibronectin adhesion, therefore tyrosine phosphorylation of FAK was investigated in DEP-1-expressing cells. Unstimulated control 1A2 cells showed only low/basal levels of FAK tyrosine phosphorylation in suspension. This increased dramatically after plating onto fibronectin (Fig. 5C) and was unaffected by mifepristone treatment. A similar pattern of FAK tyrosine phosphorylation was found in uninduced 2D3 cells. However, when DEP-1 was induced these cells showed a substantially reduced level of FAK tyrosine phosphorylation compared with 1A2 cells after plating on to fibronectin (Fig. 5C). These results indicate that both c-*src*-mediated signalling and FAK-mediated cytoskeletal events may be regulated by DEP-1.

Cytoskeletal changes associated with DEP-1 expression

Aberrant adhesion and spreading on fibronectin suggested cytoskeletal defects in DEP-1-expressing cells, so the organisation of the cytoskeletal proteins F-actin, tubulin, vinculin and paxillin was investigated. Uninduced cells displayed well-formed F-actin containing microfilament bundles within the cytoplasm and under the plama membrane. However, cells expressing DEP-1 were smaller, more rounded and contained few, if any, microfilament bundles (Fig. 6 top row). These cells also contained brightly-staining F-actin aggregates. DEP-1 expression also resulted in aberrant microtubule organisation. Whilst uninduced or control cells had well-developed microtubule networks, extending to the periphery of the cell, cells expressing DEP-1 had a less extensive microtubule netrwork, with fewer microtubules. These cells commonly contained perinuclear condensations of disorganised microtubule bundles (Fig. 6 second row). DEP-1 expression also resulted in a decrease in focal adhesion formation as assessed by paxillin and vinculin staining. Uninduced cells displayed a large number of prominent paxillin or vinculin-containing focal adhesions at the cell periphery (Fig. 6 third and fourth rows). After 48 hours of DEP-1 expression, there were virtually no paxillin-containing focal contacts in the 2C2 or 2D3 cells although they were present in the control, mifepristone-treated 1A2 cells (Fig. 6).

Focal adhesions in DEP-1-expressing cells

The observation that there were fewer vinculin and paxillin-containing focal adhesions in DEP-1-expressing cells (Fig. 6), suggested that this was the structural basis underlying the defective cell interaction with substrata such as fibronectin (Fig. 5B). Interference reflection microscopy of living cells revealed that cells in which DEP-1 was induced had aberrant substratum adhesions. Whilst the control cells were able to generate well-defined, stable focal contacts with associated stress fibres, adhesions in the DEP-1-expressing cells remained as more dot-like peripheral structures (Fig. 7A) reminiscent of focal complexes (Small, 2002). Quantification of the turnover of adhesions as a persistence index (Fig. 7B) confirmed that these attachments were transient and did not stabilise into mature focal adhesions.

DEP-1 results in defective chemotaxis

Fibroblasts have the ability to sense gradients of PDGF and

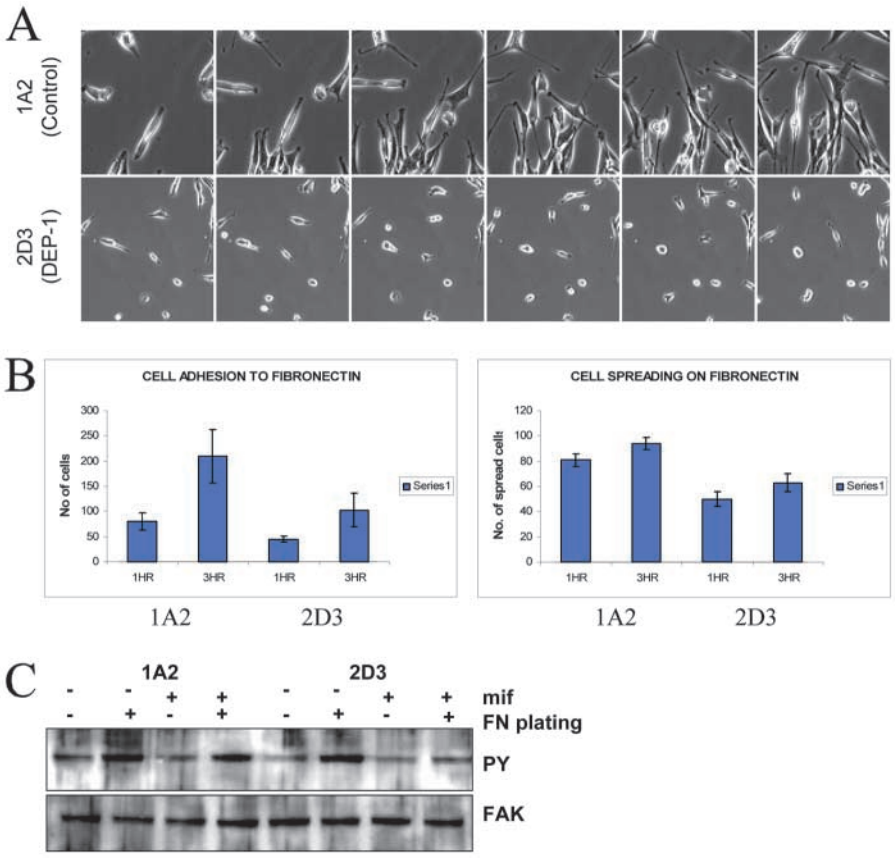

Fig. 5. DEP-1-expressing cells exhibit defective motility and interaction with fibronectin. (A) Parallel cultures of 1A2 and 2D3 cells imaged at 1-hour intervals over 6 hours showing lack of cell spreading in DEP-1-expressing 2D3 cells. (B) Quantification of cell adhesion and spreading on a fibronectin substratum. Cells were plated on to fibronectin-coated coverslips and washed after either 1 hour or 3 hours, as indicated, before fixation and counting. (C) Tyrosine phosphorylation of FAK. Cells were plated on fibronectin (FN plating +) or held in suspension (FN plating –). Lysates were immunoprecipitated with anti-FAK antibody followed by immunoblotting with anti-phosphotyrosine (upper panel) or ant-FAK (lower panel).

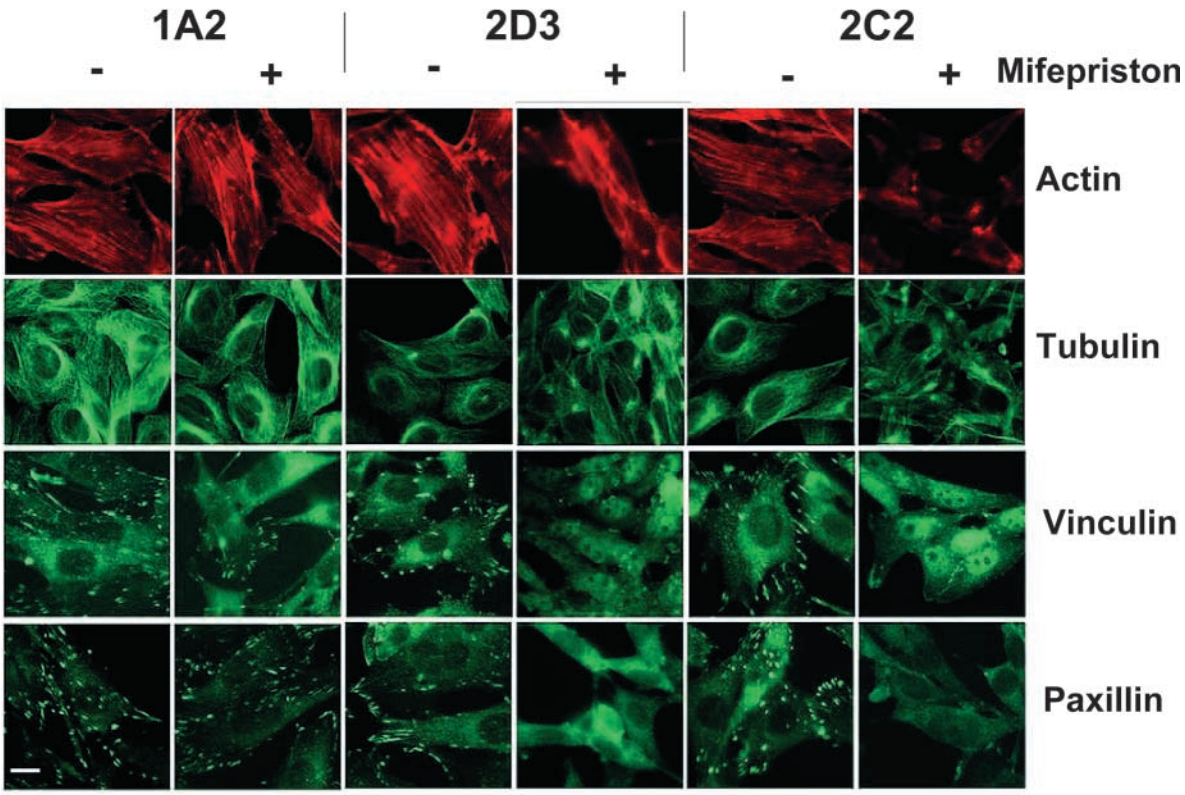

Fig. 6. Localization of cytoskeletal proteins in DEP-1-expressing cells. Control 1A2, or DEP-1-expressing 2C2 or 2D3 cells were induced with mifepristone for 24 hours, plated on to coverslips and stained for F-actin, tubulin, vinculin or paxillin as described in Materials and Methods. All of the DEP-1-expressing cells showed disruption of microfilament bundles, microtubules and adhesion plaques. Scale bar: 10 μm

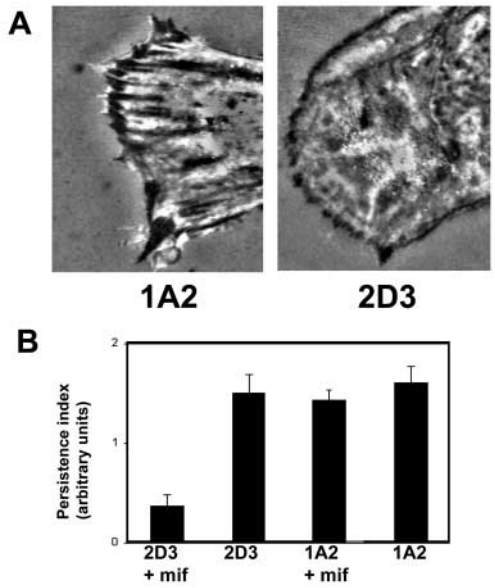

Fig. 7. Defective turnover of focal contacts in DEP-1-expressing cells. (A) Large well-developed focal contacts can be seen at the leading edge of control fibroblasts. DEP-1 expression results in cells that generate only small focal adhesions, possibly focal complexes, at the very margins of the leading lamellipodium. (B) The unstable nature of these adhesions was quantified as described and is shown as a persistence index in which a high persistence directly equates to stability of the adhesions. Mean persistence index ± s.e.m.; Student's paired *t*-test shows no significant differences between 1A2 cells plus or minus treatment with mifepristone, and $P<0.01$ between control 2D3 cells and 2D3 plus mifepristone.

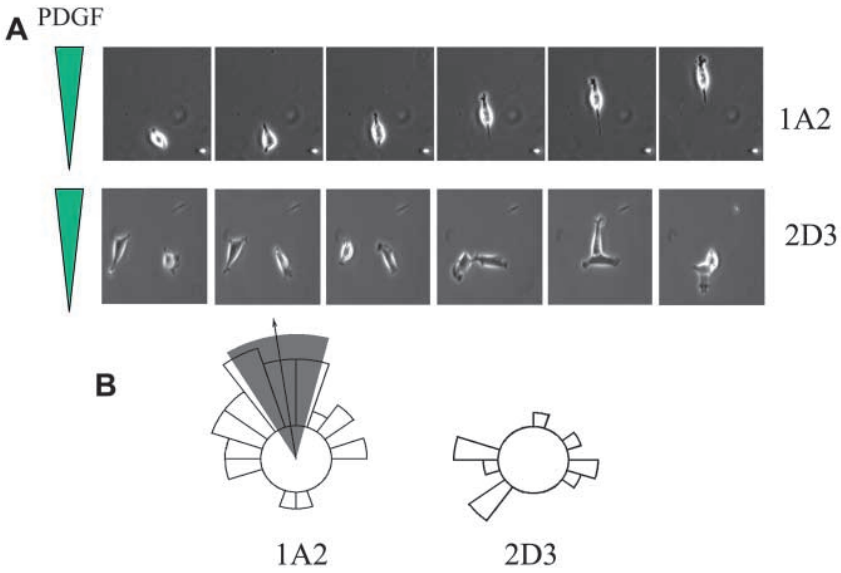

Fig. 8. Aberrant chemotaxis in DEP-1-expressing NIH3T3 cells. Cells were placed in Dunn chambers and a gradient of PGDF introduced. Cell motility was recorded by time-lapse videomicroscopy. (A) Parallel cultures of control 1A2 and DEP-1-expressing 2D3 cells imaged at 10-minute intervals for the first 60 minutes of a 6-hour chemotaxis assay. 1A2 cells migrate up the PDGF gradient, while 2D3 cells do not. (B) Horizon plots of 1A2 and 2D3 cell populations analysed for directional migration over the full 6-hour period of the assay. Significant unimodal clustering of cell directions is seen in the 1A2 population (arrow plus 95% confidence limit). As the mean direction of cell movement is upward, we conclude that 1A2 cells show positive chemotaxis to a source of PDGF (n=25 cells, taken from three separate experiments in each case).

migrate chemotactically towards the gradient source. Since proliferation in response to PDGF was diminished in DEP-1-expressing cells, we investigated whether PDGF-induced migration was also affected. Mifepristone-treated control 1A2 or DEP-1-expressing 2D3 cells were assembled on a Dunn chamber and PDGF was infused from the periphery to generate a gradient. The cells were then studied using time-lapse photography as described in Materials and Methods. 1A2 cells initially showed stimulated membrane ruffling and lamellipodia formation, followed by directed locomotion towards the gradient source. In contrast, 2C2 cells showed little stimulation of membrane activity and no directed locomotion up the PDGF gradient. Time-lapse images of the two cell types are shown in Fig. 8A, where the image interval is 10 minutes. Fig. 8B presents the Raleigh test for directional migration (Jones et al., 2000) that shows significant chemotaxis of control 1A2 cells towards PDGF. The migratory abilities of the DEP-1-expressing 2C2 cells was severely compromised, and 25 cells passing beyond the 20 μm horizon did not show any preferential directional bias.

Changes in cell-cell interactions associated with DEP-1 expression

DEP-1 induction resulted in 3T3 cells tendending to clump together, rather than attach to the tissue culture surface. Although this might be due to altered substratum adhesions or actin cytoskeleton (Figs 5 and 6), it is possible that other mechanisms might also be disrupted by DEP-1. Candidate molecules that DEP-1 might deregulate are cadherins, which are involved in intercellular interactions. Cadherin staining in mifepristone-treated 1A2 cells showed typical concentration at cell-cell contacts where plasma membranes intercalate. In these contacts the cadherin had a speckled distribution at the two interposing membranes and co-localised with high F-actin concentrations (Fig. 9, arrows). Other areas of the membranes not involved in cell-cell contact exhibited lower cadherin staining levels (Fig. 9). Cadherin staining in mifepristone-treated, DEP-1-expressing 2D3 cells, however, showed an altered localization. Whilst there was no evidence for intercalation of plasma membranes, there was strong cadherin staining along the plasma membranes of the clumped cells. Strong staining was also observed in areas of the membrane not in contact with other cells (Fig. 9 arrowhead). Western blotting showed no changes in the amount of cadherin in the cells (data not shown). β-catenin staining mimicked that of cadherin staining (Fig. 10). In the control 1A2 cells β-catenin staining appeared at discrete cell-cell junctions and areas of interposing membranes. However, in the DEP-1-expressing cells there was extensive staining along the cell peripheries where the DEP-1-expressing membranes were in contact (Fig. 10).

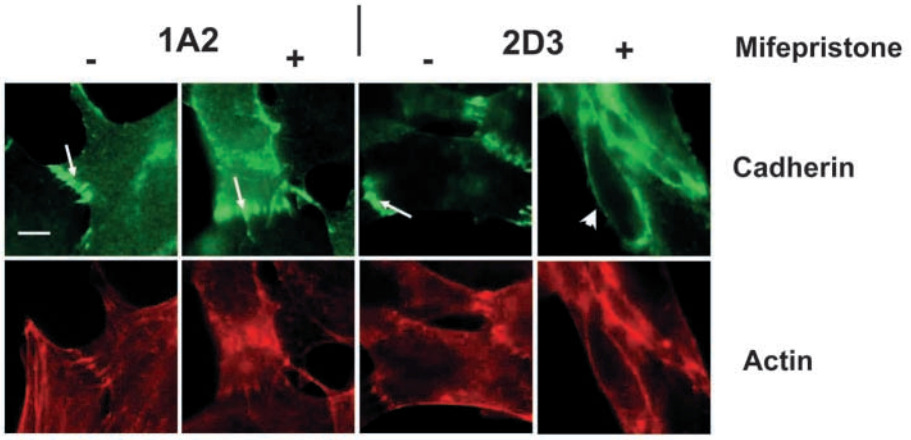

Fig. 9. Cell islands overexpressing DEP-1 have enhanced plasma membrane staining for cadherin. Control cells or DEP-1 cells were induced with mifepristone and double stained for cadherin (upper panels) and F-actin (lower panels). Uninduced cells show discrete cadherin staining at cell-cell contacts with little staining on the rest of the plasma membrane (arrows), whereas DEP-1-expressing cells show distinct staining along large areas of the membrane (arrowhead). Scale bar: 10 μm.

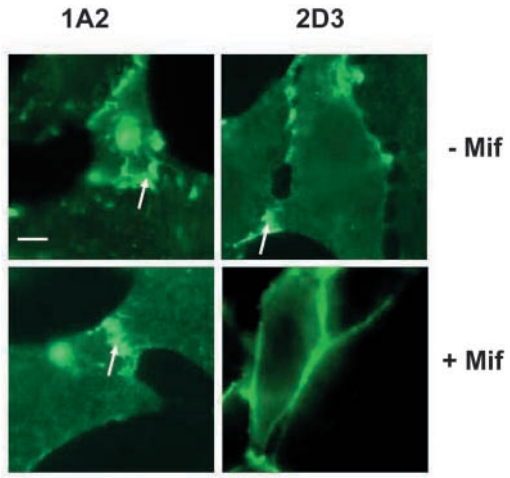

Fig. 10. Cell islands overexpressing DEP-1 accumulate β-catenin at the cell membrane. Control 1A2 cells or 2D3 DEP-1-expressing cells were induced with mifepristone and stained for β-catenin. Staining for β-catenin closely paralled that of cadherin, with uninduced cells showing discrete foci of staining at cell-cell junctions and areas of membrane intercalation (arrows). DEP-1 expressing cells showed distinct β-catenin staining along the length of the plasma membrane. Scale bar: 10 μm.

Discussion

Ostman et al. (Ostman et al., 1994) originally reported that DEP-1 expression in epithelial cells correlated with a loss of proliferative capacity. Subsequently, DEP-1 expression has been shown to inhibit cancer cell growth, to dephosphorylate the PDGF receptor and to associate with $p120^{ctn}$ in different cell types (Keane et al., 1996; Kovalenko et al., 2000; Holsinger et al., 2002). We found that inducible DEP-1 expression in fibroblasts leads to decreases in proliferation concurrent with defective cell-substratum contacts, FAK phosphorylation and cadherin distribution. Cell proliferation experiments demonstrated that ectopic expression of DEP-1 in NIH3T3 cells caused cell cycle arrest, with a dramatic reduction in the population of cells in the synthetic phase of the cell cycle under normal growth conditions. Previous attempts to generate stable cell lines overexpressing DEP-1 had failed because of a lack of growth in selection media, and it seems reasonable to conclude that the reason for this was failure of the DEP-1-expressing cells to proliferate. To further investigate the role of DEP-1 in proliferation responses, cells were made quiescent and then stimulated with PDGF. Whilst mifepristone-treated control cells showed increased cellular tyrosine phosphorylation in response to PDGF, mifepristone-induced DEP-1 cells showed no such increases. Ligand-induced PDGF receptor phosphorylation was also substantially reduced in DEP-1-expressing cells. This supports previous reports that the PDGF receptor is a substrate for DEP-1 (Kovalenko et al., 2000; Persson et al., 2002). Since ligand-induced PDGF receptor phosphorylation was prevented in DEP-1-overexpressing cells, it is probable that downstream signalling events controlled by this would be inhibited. Reduced tyrosine phosphorylation of PDGF in DEP-1-expressing cells was consistent with a failure of c-*src* to associate with the activated PDGF receptor, implying that the c-*src* recognition site was dephosphorylated by DEP-1. Cells expressing DEP-1 also showed a reduction in phosphorylation of p42/44 MAPK and akt/PKB. These results indicate that DEP-1 antagonizes the PDGF receptor kinase activity and prevents signalling through the c-*src*, ras-MAPK and PI 3-kinase-Akt pathways at the level of receptor activation. It is probable that increased DEP-1 expression and activity is responsible for the reduction in proliferation, rather than cell-cell contact per se, as under the subconfluent conditions applied here only a small proportion of the cells were in cell-cell contact.

Overexpression of DEP-1 in 3T3 cells resulted in distinct morphological changes, with cells being more rounded and phase-bright. To define this observation in more detail, cell adhesion and spreading on a fibronectin substratum was quantified, with DEP-1-expressing cells showing a significant reduction in the ability to both adhere and spread. Immunofluorescence showed that F-actin-containing stress fibres were reduced in DEP-1-expressing cells, with a concomitant increase in F-actin at the cell membrane, and gross changes to the microtubule-based cytoskeleton. We do not know as yet whether the alteration in microtubule organisation is a direct consequence of actin fibre dissolution or is an independent variable of DEP-1 expression. There was also a reduction in vinculin and paxillin-containing focal adhesions. IRM experiments on living cells showed that these abnormalities were due to the inability of punctate focal adhesions in DEP-1-expressing cells to mature into larger, stable adhesion plaques (focal contacts). There is some

evidence that stress fibres condense on focal adhesion assemblies, and so the lack of stress fibres in DEP-1-positive cells may be a result of the failure of focal complexes to mature into focal contacts. Tyrosine phosphorylation of FAK was dramatically reduced in DEP-1-expressing cells, and this may be one mechanism by which these cells fail to produce mature focal contacts, since phosphorylation of FAK and $p130^{cas}$ is essential for focal adhesion assembly and turnover. In support of this, $p130^{cas}$ has recently been shown to be a substrate of the DEP-1-related phosphatase SAP-1 (Noguchi et al., 2001). DEP-1-expressing cells also failed to show a normal chemotactic response towards a PDGF source. It may be that this defective migration is also due to failure in cell substratum adhesions, although time-lapse videos showed that these cells frequently failed to extend initial lamellipodia in the direction of the gradient, suggesting a primary defect in gradient sensing and response, a cell polarisation property intimately linked to PI 3-kinase-mediated transduction pathways (Wang et al., 2002; Weiner et al., 2002; Funamoto et al., 2002; Comer et al., 2002). We have shown that at least one PI 3-kinase pathway (activation of Akt) is inhibited by DEP-1 expression, and further work should clarify the role of DEP-1 in modulating directed cell translocation. GLEPP-1 (a member of the DEP-1 subfamily) overexpression in macrophages also results in disruption of focal contacts and cytoskeletal components (Pixley et al., 2001). FAK activation is a common point of convergence between growth factors and substratum adhesion and thus may be a major substrate for DEP-1 that regulates both these events.

Surprisingly, DEP-1 expression enhanced cell-cell adhesion. This appeared to be not just the result of decreased cell-substratum adhesion, but of a defined molecular mechanism. In control cells, cell-cell contacts occurred at small discrete areas of the plasma membrane and these stained strongly for cadherin where the plasma membranes intercalated, with much lower levels observed in other areas of the plasma membrane. In contrast, DEP-1-expressing cells clustered together and displayed extended contacts, which stained strongly for cadherin over large areas of the plasma membrane. These data are consistent with an increase in the adherens junction structure(s) in DEP-1-expressing cells such that the intercellular contacts are more reminiscent of the continuous adherens junctions found in epithelial cells. Thus overexpression of DEP-1 may result in increased organisation of cell-cell junctions. Although we cannot formally differentiate between cause and effect of increased cadherin and increased cell clustering, the increased staining of cadherin occurred in areas of the plasma membrane not in contact with other cells, thus increased cadherin at the plasma membrane is independent of intercellular cadherin clustering. Holsinger et al. (Holsinger et al., 2002) have shown that DEP-1 associated with $p120^{ctn}$ in A431 epithelial carcinoma cells, and our results are in broad agreement with Lampugnani et al. (Lampugnani et al., 2003) who reported that contact inhibition of VEGF-induced proliferation requires DEP-1 as well as endothelial cadherin and β-catenin. RPTPμ has also been shown to dephosphorylate $p120^{ctn}$, so it is possible that different members of the PTP family have overlapping functions (Zondag et al., 2000). Whilst our results indicate that the PDGF receptor is a direct substrate for DEP-1, it is possible that the antiproliferative effects seen are an indirect consequence of β-catenin translocation. For example, there was also an increase in the intensity of membrane staining for β-catenin, suggesting that increased membrane cadherin recruited β-catenins, and thus could be part of a signalling complex. If β-catenins were sequestered to the plasma membrane then there would be a reduction in the pool of these molecules available for cytoplasmic-nuclear translocation, and therefore a reduction in β-catenin-associated transcription factor activity. This in turn could downregulate the proliferative activity of the cells. Several other PTPs such as LAR and PTPμ/κ have also been implicated in cadherin and β-catenin regulation (Aicher et al., 1997; Kypta et al.., 1996; Brady-Kalnay et al., 1995; Fuches et al., 1996), and recently PTPα has been shown to regulate integrin-stimulated FAK autophosphorylation and cytoskeletal rearrangements (Zeng et al., 2003).

It is now apparent that PTPs can have specific and selective roles in cell regulation. Although some PTPs such as PTPα and CD45 have positive roles, the majority appear to have negative regulatory roles in cell function (Andersen et al., 2001). This is perhaps best exemplified by PTP1B, which is a negative regulator of insulin receptor signalling; indeed PTP1B inhibitors are in various phases of clinical trials as antidiabetic therapeutics (Johnson et al., 2002). Other examples of antagonistic effects towards growth factors include SHP-2, LAR, PTPσ, TCPTP (Klinghoffer and Kazlauskas, 1995; Kulas et al., 1996; Suares-Pestana et al., 1999; Tiganis et al., 1998; Koslowski et al., 1998). DEP-1 appears to belong to a subfamily that controls tyrosine kinase receptor-mediated cellular proliferation and cytoskeletal regulation, and thus is a crucial molecule for many growth factor-mediated cellular responses.

We thank Jane Clarkson and Ming Chang for helpful advice on gene expression analysis and western blotting. This work was partly funded by a grant from University of Queensland and the CRC for Chronic inflammatory diseases.

References

Aicher, B., Lerch, M. M., Muller, T., Schilling, J. and Ullrich, A. (1997). Cellular redistribution of protein tyrosine phosphatases LAR and PTPsigma by inducible proteolytic processing. *J. Cell Biol.* **138**, 681-696.

Allen, W. E., Zicha, D., Ridley, A. J. and Jones, G. E. (1998). A role for Cdc42 in macrophage chemotaxis. *J. Cell Biol.* **41**, 1147-1157.

Andersen, J. N., Mortensen, O. H., Peters, G. H., Drake, P. G., Iversen, L. F., Olsen, O. H., Jansen, P. G., Andersen, H. S., Tonks, N. K. and Moller, N. P. (2001). Structural and evolutionary relationships among protein tyrosine phosphatase domains. *Mol. Cell. Biol.* **21**, 7117-7136.

Autschbach, F., Palou, E., Mechtersheimer, G., Rohr, C., Pirotto, F., Gassler, N., Otto, H. F., Schraven, B. and Gaya, A. (1999). Expression of the membrane protein tyrosine phosphatase CD148 in human tissues. *Tissue Antigens* **54**, 485-498.

Baker, J. E., Majeti, R., Tangye, S. G. and Weiss, A. (2001). Protein tyrosine phosphatase CD148-mediated inhibition of T-cell receptor signal transduction is associated with reduced LAT and phospholipase Cgamma1 phosphorylation. *Mol. Cell. Biol.* **21**, 2393-2403.

Billard, C., Delaire, S., Raffoux, E., Bensussan, A. and Boumsell, L. (2000). Switch in the protein tyrosine phosphatase associated with human CD100 semaphorin at terminal B-cell differentiation stage. *Blood* **95**, 965-972.

Binstadt, B. A., Brumbaugh, K. M., Dick, C. J., Scharenberg, A. M., Williams, B. L., Colonna, M., Lanier, L. L., Kinet, J. P., Abraham, R. T. and Leibson, P. J. (1996). Sequential involvement of Lck and SHP-1 with MHC-recognizing receptors on NK cells inhibits FcR-initiated tyrosine kinase activation. *Immunity* **5**, 629-638.

Brady-Kalnay, S. M., Rimm, D. L. and Tonks, N. K. (1995). Receptor protein tyrosine phosphatase mu associates with cadherins and catenins in vivo. *J. Cell Biol.* **130**, 977-986.

Chen, H. E., Chang, S., Trub, T. and Neel, B. G. (1996). Regulation of colony-stimulating factor 1 receptor signaling by the SH2 domain-containing tyrosine phosphatase SHPTP1. *Mol. Cell. Biol.* **16**, 3685-3697.

Comer, F. I. and Parent, C. A. (2002). PI 3-kinases and PTEN: how opposites chemoattract. *Cell* **10**, 541-544.

de la Fuente-Garcia, M. A., Nicolas, J. M., Freed, J. H., Palou, E., Thomas, A. P., Vilella, R., Vives, J. and Gaya, A. (1998). CD148 is a membrane protein tyrosine phosphatase present in all hematopoietic lineages and is involved in signal transduction on lymphocytes. *Blood* **9**, 2800-2809.

del Pozo, V., Pirotto, F., Cardaba, B., Cortegano, I., Gallardo, S., Rojo, M., Arrieta, I., Aceituno, E., Palomino, P., Gaya, A. and Lahoz, C. (2000). Expression on human eosinophils of CD148: a membrane tyrosine phosphatase. Implications in the effector function of eosinophils. *J. Leukoc. Biol.* **68**, 31-37.

Elchebly, M., Payette, P., Michaliszyn, E., Cromlish, W., Collins, S., Lot, A. L., Normandin, D., Cheng, A., Himms-Hagen, J., Chan, C. C., Ramachandran, C., Gresser, M. J., Tremblay, M. L. and Kennedy, B. P. (1999). Increased insulin sensitivity and obesity in mice lacking the protein tyrosine phosphatase PTP1B gene. *Science* **283**, 1544-1548.

Flint, A. J., Tiganis, T., Barford, D. and Tonks, N. K. (1997). Development of substrate-trapping mutants to identify physiological substrates of protein tyrosine phosphatases. *Proc. Natl. Acad. Sci. USA* **94**, 1680-1685.

Fuchs, M., Muller, T., Lerch, M. M. and Ullrich, A. (1996). Association of human protein-tyrosine phosphatase kappa with members of the armadillo family. *J. Biol. Chem.* **271**, 16712-16719.

Funamoto, S., Meili, R., Lee, S., Parry, L. and Firtel, R. A. (2002). Spatial and temporal regulation of 3-phosphoinositides by PI 3-kinase and PTEN mediates chemotaxis. *Cell* **109**, 611-623.

Holsinger, L. J., Ward, K., Duffield, B., Zachwieja, J. and Jallal, B. (2002). The transmembrane receptor protein tyrosine phosphatase DEP1 interacts with $p120^{ctn}$. *Oncogene* **21**, 7067-7076.

Hubbard, S. R. and Till, J. H. (2000). Tyrosine kinase structure and function. *Ann. Rev. Biochem*. **69**, 373-398.

Hundt, M. and Schmidt, R. E. (1997). Functional characterization of receptor-type protein tyrosine phosphatase CD148 (HPTP eta/DEP-1) in Fc gamma receptor IIa signal transduction of human neutrophils. *Eur. J. Immunol.* **27**, 3532-3535.

Johnson, T. O., Ermolieff, J. and Jirousek, M. R. (2002). Protein tyrosine phosphatase 1B inhibitors for diabetes. *Nat. Rev. Drug Discov.* **1**, 696-709.

Jones, G. E., Ridley, A. J. and Zicha, D. (2000). Rho GTPases and cell migration: measurement of macrophage chemotaxis. *Methods Enzymol.* **325**, 449-462.

Keane, M., Lowrey, G. A., Ettenberg, S. A., Dayton, M. A. and Lipkowitz, S. (1996). The protein-tyrosine phosphatase DEP-1 is induced during differentiation and inhibits the growth of breast cancer cells. *Cancer Res.* **56**, 4236-4243.

Klinghoffer, R. A. and Kazlauskas, A. (1995). Identification of a putative Syp substrate, the PDGFβ receptor. *J. Biol. Chem.* **270**, 22208-22217.

Koslowski, M., Larose, L., Lee, F., Le, D. M., Rottapel, T. and Siminovitch, K. A. (1998). SHP-1 binds and negatively regulates the c-kit receptor by interaction with tyrosine 569 in the c-kit juxtamembrane domain. *Mol. Cell. Biol.* **18**, 2089-2099.

Kovalenko, M., Denner, K., Sandstrom, J., Persson, C., Gross, S., Jandt, E., Vilella, R., Bohmer, F. and Ostman, A. (2000). Site-selective dephosphorylation of the platelet-derived growth factor beta-receptor by the receptor-like protein-tyrosine phosphatase DEP-1. *J. Biol. Chem.* **275**, 16219-16226.

Kulas, D. T., Zhang, W. R., Goldstein, B. J. and Mooney, R. A. (1996). The transmembrane protein-tyrosine phosphatase LAR modulates signalling by multiple receptor tyrosine kinases. *J. Biol. Chem.* **271**, 748-754.

Kypta, R. M., Su, H. and Reichardt, L. F. (1996). Association between a transmembrane prorein tyrosine phosphatase and the cadherin-catenin complex. *J. Cell Biol.* **134**, 1519-1529.

Mardia, K. V. (1972). *Statistics of Directional Data.* pp. 1-357. New York: Academic Press.

Murray, J. T. C., Craggs, G., Wilson, L. and Kellie, S. (2000). Mechanism of PI 3-kinase-dependent increases in macrophage cell density in response to M-CSF. *Inflammation Research* **49**, 610-618.

Noguchi, T., Tsuda, M., Takeda, H., Takada, T., Inagaki, K., Yamao, T., Fukunaga, K., Matozaki, T. and Kasuga, M. (2001). Inhibition of cell growth and spreading by stomach cancer-associated protein-tyrosine phosphatase-1 (SAP-1) through dephosphorylation of p130cas. *J. Biol. Chem.* **276**, 15216-15224.

Lampugnani, M. G., Zanetti, A., Corada, M., Takahashi, T., Balconi, G., Brevario, F., Orsenigo, F., Cattelino, A., Kemler, R., Daniel, T. O. and Dejana, E. (2003). Contact inhibition of VEGF-induced proliferation requires vascular cadherin, β-catenin, and the phosphatase DEP-1/CD148. *J. Cell Biol.* **161**, 793-804.

Osborne, J. M., den Elzen, N., Lichanska, A. M., Costelloe, E. O., Yamada, T., Cassady, A. I. and Hume, D. A. (1998). Murine DEP-1, a receptor protein tyrosine phosphatase, is expressed in macrophages and is regulated by CSF-1 and LPS. *J. Leukoc. Biol.* **64**, 692-701.

Ostman, A., Yang, Q. and Tonks, N. K. (1994). Expression of DEP-1, a receptor-like protein-tyrosine-phosphatase, is enhanced with increasing cell density. *Proc. Natl. Acad. Sci. USA* **91**, 9680-9684.

Östman, A. and Böhmer, F. D. (2001). Regulation of receptor tyrosine kinase signaling by protein tyrosine phosphatases. *Trends Cell Biol*. **11**, 258-266.

Palou, E., de la Fuente-Garcia, M. A., Nicolas, J. M., Vilardell, C., Vives, J. and Gaya, A. (1997). CD148, a membrane protein tyrosine phosphatase, is able to induce tyrosine phosphorylation on human lymphocytes. *Immunol. Lett.* **57**, 101-103.

Persson, C., Engstrom, U., Mowbray, S. L. and Ostman, A. (2002). Primary sequence determinants responsible for site-selective dephosphorylation of the PDGF beta-receptor by the receptor-like protein tyrosine phosphatase DEP-1. *FEBS Lett.* **517**, 27-31.

Pixley, F. J., Lee, P. W. S., Condeelis, J. and Stanley, E. R. (2001). Protein tyrosine phosphatase phi regulates paxillin tyrosine phosphorylation and mediates colony-stimulating factor 1 induced morphological changes in macrophages. *Mol. Cell. Biol.* **21**, 1795-1809.

Rivenkamp, A. L., van Wezel, T., Zanon, C., Stassen A. P. M. et al. (2002). *PTPRJ* is a candidate for the mouse colon-cancer susceptibility locus Scc1 and is frequently deleted in human cancers. *Nature Genet.* **31**, 295-300.

Schlessinger, J. (2000). Cell signalling tyrosine kinases. *Cell* **103**, 211-225.

Small, J. V., Stradal, T., Vignal, E. and Rottner, K. (2002). The lamellipodium: where motility begins. *Trends Cell Biol.* **12**, 112-120.

Sorby, M. and Ostman, A. (1996) Protein-tyrosine phosphatase-mediated decrease of epidermal growth factor and platelet-derived growth factor receptor tyrosine phosphorylation in high cell density cultures. *J. Biol. Chem.* **271**, 10963-10966.

Sturge, J., Hamelin, J. and Jones, G. E. (2002). N-WASP activation by a beta1-integrin-dependent mechanism supports PI3K-independent chemotaxis stimulated by urokinase-type plasminogen activator. *J. Cell Sci.* **115**, 699-711.

Suares-Pestana, E., Tenev, T., Gross, S., Stoyanov, B., Ogata, M. and Bohmer, F. D. (1999). The transmembrane protein tyrosine phosphatase RPTPsigma modulates signalling of the epidermal growth factor receptor in A431 cells. *Oncogene* **18**, 4069-4079.

Tangye, S. G., Phillips, J. H., Lanier, L. L., de Vries J. E. and Aversa, G. (1998a). CD148: a receptor-type protein tyrosine phosphatase involved in the regulation of human T cell activation. *J. Immunol.* **161**, 3249-3255.

Tangye, S. G., Wu, J., Aversa, G., de Vries J. E., Lanier, L. L. and Phillips, J. H. (1998b). Negative regulation of human T cell activation by the receptor-type protein tyrosine phosphatase CD148. *J. Immunol.* **161**, 3803-3807.

Tiganis, T., Kemp, B. and Tonks, N. K. (1999). The protein-tyrosine phosphatase TCPTP regulates epidermal growth factor receptor-mediated signalling and phosphatidylinositol3-kinase-dependent signalling. *J. Biol. Chem.* **274**, 27768-27775.

Wang, F., Herzmark, P., Weiner, O. D., Srinivasan, S., Servant, G. and Bourne, H. R. (2002). Lipid products of PI(3)Ks maintain persistent cell polarity and directed motility in neutrophils. *Nat. Cell Biol.* **4**, 513-518.

Weiner, O. D., Neilsen, P. O., Prestwich, G. D., Kirschner, M. W., Cantley, L. C. and Bourne, H. R. (2002). A PtdInsP(3)- and Rho GTPase-mediated positive feedback loop regulates neutrophil polarity. *Nat. Cell Biol.* **4**, 509-513.

Wilson, L., Carrier, M. and Kellie, S. (1995). $pp125^{FAK}$ tyrosine kinase activity is not required for the assembly of stress fibres and focal adhesions in cultured mouse aortic smooth muscle cells. *J. Cell Sci.* **108**, 2381-2391.

Zeng, L., Si, X., Yu, W. P., Le, H. T., Ng, K. P., Teng, R. M. H., Ryan, K., Wang, D. Z. M., Ponniah, S. and Pallen, C. J. (2003). PTP regulates integrin-stimulated FAK autophosphorylation and cytoskeletal rearrangement in cell spreading and migration. *J. Cell Biol.* **160**, 137-146.

Zicha, D., Dunn, G. A. and Brown, A. F. (1991). A new direct-viewing chemotaxis chamber. *J. Cell Sci.* **99**, 769-775

Zondag, G. C., Reynolds, A. B. and Moolenaar, W. H. (2000). Receptor protein-tyrosine phosphatase RPTPmu binds to and dephosphorylates the catenin p120(ctn). *J. Biol. Chem.* **275**, 11264-11269.